Comparison of Finite Element and Monte Carlo Simulations for Inhomogeneous Advanced Breast Cancer Imaging

Yan Xu* and Quing Zhu
Department of electrical and Computer engineering, University of Connecticut
*Corresponding author: 371 Fairfield Way; U2157, Storrs, CT, 06269, USA. yax08001@engr.uconn.edu

Abstract: Tumor vascular patterns of advanced breast cancers are complex and heterogeneous. Near infrared (NIR) optical tomography has great potential to image tumor vascular and hypoxia patterns. The simulation of NIR diffusion in turbid tissue is indispensable to accelerate the practice in clinic. In this article, the two popular simulation methods, Finite element (FEM) and Monte Carlo (MC), are compared towards running time, reconstruction results and accuracy ratio. Three-dimensional FEM method provided by Comsol is used to model an inhomogeneous advanced breast tumor of different optical properties for outer layer and inner core in a semi-infinite medium. The MC simulation developed by standard C modeled the same condition using 30 million photons. The phantom experiment in similar condition using ultrasound-guided NIR imaging system is also performed to verify the simulations.

Keywords: Finite Element. Monte Carlo. optical tomography. advanced breast cancer imaging.

1. Introduction

Tumor vasculature is directly related to tumor proliferation, growth, and metastasis; while tumor hypoxia alters the pattern of gene expression leading to more aggressive behavior with increased metastatic potential and treatment resistance. However, the process of tumor angiogenesis is complex resulting in a highly distorted and heterogeneous distribution of blood vessels in advanced cancers. NIR optical tomography has tremendous potential to provide clinically useful functional information about tumor angiogenesis and tumor hypoxia[1-4]. The FEM[5-6] and MC[7-8], two popular simulation methods, are used to simulate the inhomogeneous advanced breast tumor in turbid medium. The FEM is provided by Comsol and MC is developed by standard C. The corresponding phantom experiment is performed as validation.

2. Finite Element method

2.1 Diffusion Equation

The diffusion theory is widely proved to be used to calculate photon migration in biological tissues. There are two important approximations for diffusion theory, (1). The source-detector separation is much greater than the random walk mean free path; (2). The reduced scatter coefficient (μ_s') is greatly larger than the absorption coefficient (μ_a). The temporal diffusion equation in highly scattering media could be depicted as:

$$\frac{1}{v}\frac{\partial}{\partial t}U(\vec{r},t) - D\nabla^2 U(\vec{r},t) + \mu_a U(\vec{r},t) = S(\vec{r},t) \qquad (1)$$

where $U(\vec{r},t)$ is the photon density wave at position $\vec{r}$; $D = 1/(3\mu_s')$ is the diffusion coefficient of medium; $S(\vec{r},t)$ is the point source term and v is the speed of light inside the medium. When frequency modulation (140MHz) is adopted to the point source, equation (1) can be rewritten in frequency-domain as:

$$D\nabla^2 U(\vec{r},\omega) - (\mu_a - j\frac{\omega}{v})U(\vec{r},\omega) = -S_0\delta(\vec{r}) \qquad (2)$$

which can be further simplified as Helmholtz equation:

$$(\nabla^2 + k^2)U(\vec{r}) = -\frac{S_0}{D}\delta(\vec{r}) \qquad (3)$$

where S_0 relates to the source strength, $\delta(\vec{r})$ is a delta function, ω is the modulation frequency, and $k = \sqrt{\frac{1}{D}(-\mu_a + i\frac{\omega}{v})}$ is the complex wave vector.

2.2 Model construction

COMSOL has been employed to solve the forward diffusion equation in frequency domain. This software provides users various existing models which based on partial differential equations and solve them using the FEM method with high-performance solvers. In COMSOL, the Helmholtz Equation from *Comsol Multiphysics classical PDE Modes* and Neumann type boundary condition are used to model the diffusive light propagation which expressions as following:

$$-\nabla \cdot (c\nabla u) + a \cdot u = f \quad (4)$$

$$\hat{n} \cdot (c\nabla u) + q \cdot u = g \quad (5)$$

where u corresponds to $U(\vec{r})$ in equation (3) and parameters c, a and f can also be matched to equation (3), respectively. $\hat{n}$ is the outward unit normal vector on the boundary, q is a positive number related to the internal reflection and g is the source term on the boundary. Since the matched refractive index and the absorption boundary are applied, g equals 0 and q equals 0.5.

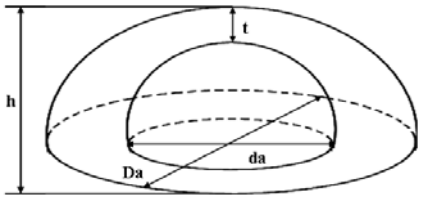

Figure 1. The geometry of the concentric semi-ellipsoidal target.

A cylinder of 20 cm diameter and 10 cm height is modeled to approximate the semi-infinite medium and a concentric semi-ellipsoidal absorber with different optical properties of outer layer and inner core are embedded in this medium, as shown in Figure 1, which closely models large breast lesions when patients are imaged in a supine position using the conventional pulse-echo ultrasound and our hand-held combined probe. In Figure 1, Da is the diameter of outer layer, da is the inner diameter of the core, t is the thickness between the outer shell and the inner core and h is the height of the semi-ellipsoid. The flat probe is located on the surface of the cylinder to shine the point sources into the medium and collect the reflected photon waves with the detectors. The data is acquired based on single source each time as Figure 2 shows.

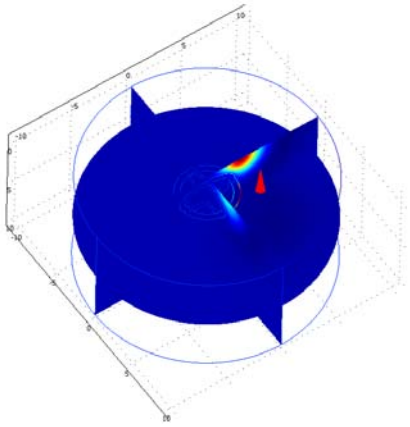

Figure 2. The visualization and illumination of the inhomogeneous large target under one source pulse.

3. Monte Carlo method

The Time-Domain MC method is used to generate the forward data with a target inside the turbid medium located at different depths. The reflection geometry with multiple sources and detectors distributed on a probe of 10 cm diameter is used in the MC simulation. At each source location, a delta pulse consisting of 30 millions of photons is lunched into the medium. Initially, each photon is assigned a unity weight W, which is analogous to light intensity. Each photon goes through many steps of absorption and scattering processes. After each step, a part of the weight ΔW is absorbed by the medium and the weight of the photon is decreased. The photon is scattered following the Henyey-Greenstein function. The Roulette technique is used to terminate the photon when the residual weight is less than a threshold value. For each photon, it is either absorbed in the medium, detected at the reflecting surface, or leaves from the transmitting surface. After the migration of one particular photon halted, a new photon is launched into the medium at the source location. Each photon's energy and arrival time are recorded when the photon reaches the outer surface (boundary). The MC program has been extended to include a large semi-ellipsoidal inhomogeneous target embedded inside a turbid medium, due to most of the large lesions are

squashed into a semi-ellipsoidal shape against the chest-wall under the slight probe compression. The boundary conditions between target layers and medium could be easily controlled by mapping corresponding refractive indexes in an input file.

4. Imaging Reconstruction

Born approximation is used to approximate the photon density wave as a linear superposition of homogeneous incident and scattering fields. The dual-zone mesh scheme which segments the imaging volume into two regions consisting of the target and the background region is used for reconstruction with the location information provided by the co-registered ultrasound image. The conjugate gradient method was used for the iterative optimization. Typically, in simulations and phantom experiments, the fine mesh region is chosen about 3-4 times larger than the true target area. This method significantly reduces the background artifacts because the voxel size in the background area is much larger than that in the target area.

5. Phantom experiment

Phantoms of different size with different optical properties were made using polyvinyl chloride-plastisol (PVCP) solution, which was a white opaque solution and became translucent when it was heated to a high temperature [9]. When the solution was gradually heated, the Indian ink and titanium dioxide (TiO2) powder were added to control the optical absorption and scattering coefficients of the phantom.

Our frequency domain system (Figure 3) consisted of 14 parallel detectors and 4 laser diodes of 740nm, 780nm, 808nm and 830nm. Each laser diode was sequentially switched to 9 positions on the probe. The center slot on the probe was used for ultrasound transducer and the sources and detectors were distributed on both sides. Intralipid solution was used to emulate the background tissue. Measurements were made with the target inside the intralipid (target data) and intralipid alone as a reference. The perturbation between the target data and the reference was used for imaging reconstruction.

Figure 3. The ultrasound-guided NIR imaging system in the operating room

6. Results

6.1 Simulation results of FEM

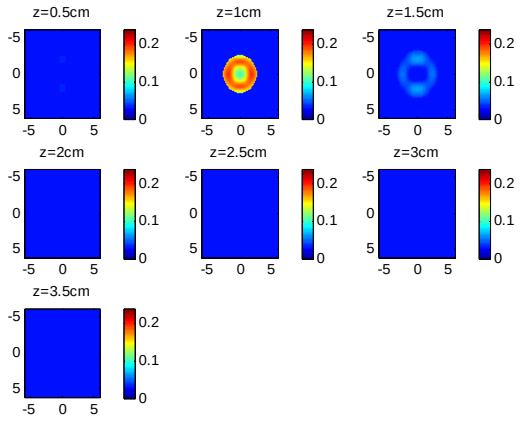

Figure 4. The FEM reconstructed image of an inhomogeneous target with outer diameter of 5 cm and inner core diameter of 2.5 cm and height of 2 cm.

A semi-ellipsoidal target presented in this set of simulation had outer diameter of 5 cm, inner core diameter of 2.5 cm, h of 2 cm and t of 0.5 cm. The target outer shell and inner core had same reduced scattering coefficient of μ_s' = 6.0 cm^{-1} and different absorption coefficients of μ_a = 0.25 cm^{-1} and μ_a = 0.06 cm^{-1}, respectively. The background optical properties were set to μ_a = 0.03 cm^{-1} and μ_s' = 6.0 cm^{-1}. After the frequency-domain data collected from 9 sources

in Comsol, respectively, the Born approximation was applied to reconstruct the images. Figure 4 showed the reconstructed absorption map of the target whose bottom was located at 2.5 cm. The maximum reconstructed absorption coefficient was 0.20 and the periphery of the target shows higher absorption than the inner core as the true structure of the inhomogeneous target.

6.2 Simulation results of MC

In MC simulation, a semi-ellipsoidal target with the same structural and optical properties as the one described in section 6.1 was conducted. Figure 5 showed the reconstructed absorption map of the target whose bottom was located at 2.5 cm. The maximum reconstructed absorption coefficient was 0.14 and the periphery of the target shows higher absorption than the inner core as Figure 4 but with lower reconstructed maximum absorption coefficient.

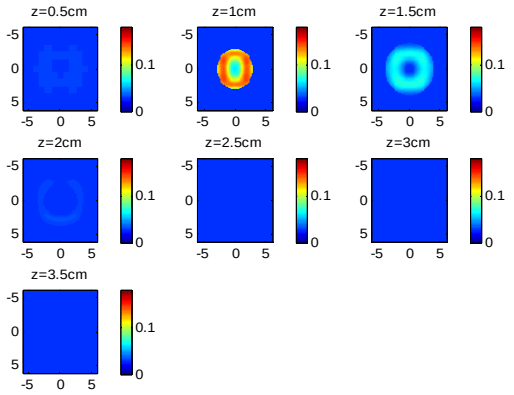

Figure 5. The MC reconstructed image of an inhomogeneous target with outer diameter of 5 cm and inner core diameter of 2.5 cm and height of 2 cm.

6.3 Comparison of FEM and MC

We compared the two simulation methods towards running time, reconstruction results and accuracy ratio. In Comsol, the running time of FEM simulation for one source and 14 detectors was 17.658s, while in MC, when 30 million photons was used, the running time was 91017s, 5154 times longer. From the reconstruction results from section 6.1 and 6.2, we could see the reconstructed images were similar for both FEM and MC methods, but the reconstructed absorption coefficient was 0.20, 80% accuracy for FEM and only 0.14, 56% accuracy for MC simulation. It is obviously, the FEM method is much more efficient and accurate than MC method.

6.4 Phantom experiments

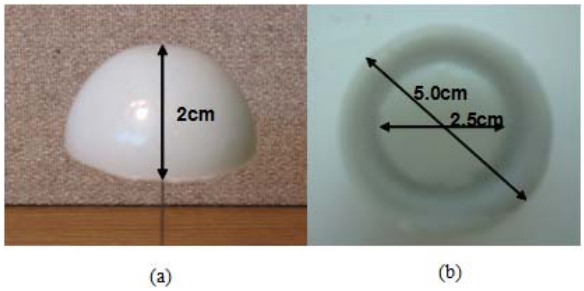

Figure 6. The structure of a concentric semi-ellipsoidal target phantom. (a) The front view of the phantom. (b) The bottom view of the phantom.

To validate the simulation results, phantom experiments with the similar condition were performed. The intralipid solution of calibrated μ_a = 0.03 cm^{-1} and μ_s' =7.2 cm^{-1} at 780 nm wavelength was used as the background. The target shown in Figure 6 had outer shell diameter of 5.0 cm, inner core diameter of 2.5 cm, height h of 2.0 cm and t of 0.5 cm. Shell had the μ_a = 0.25 cm^{-1} and μ_s' = 7.1 cm^{-1} and the core had μ_a = 0.06 cm^{-1} and μ_s' = 5.2 cm^{-1}.

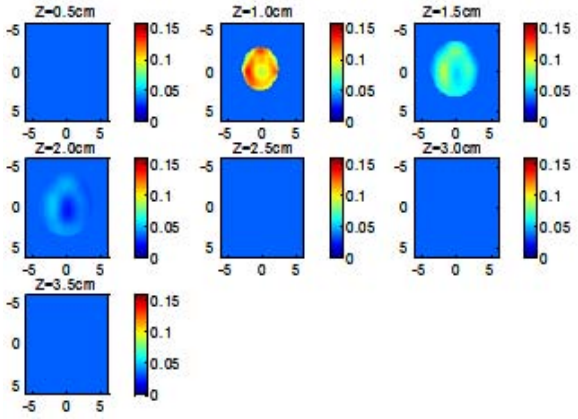

Figure 7. Phantom result of a concentric semi-ellipsoidal target with outer shell diameter of 5 cm, inner core diameter of 2.5 cm, height of 2 cm and layer thickness of 0.5 cm. The target bottom was located at 2.5 cm.

Figures 7 shows the reconstructed absorption map when the bottom of the target was located at the 2.5 cm. The reconstructed maximum μ_a was 0.15 cm^{-1}. The periphery enhancement was showed similarly as that in the images of simulations, which verify the results we gained in both FEM and MC simulations.

7. Conclusions

We compared the performance between FEM simulation provided by Comsol and the MC simulation developed by standard C towards running time, reconstructed results and the accuracy ratio. The results from both simulation and experiment validated that NIR optical tomography could resolve the inhomogeneous advanced tumor and the FEM method from Comosl could offer the simulation with higher efficiency and accuracy.

8. References

1. B. J. Tromberg, A. Cerussi, et al, "Imaging in breast cancer: diffuse optics in breast cancer: detecting tumors in pre-menopausal women and monitoring neoadjuvant chemotherapy," *Breast Cancer Res*. **7**(6), 279-85 (2005)
2. B. Chance, S. Nioka, et al, "Breast Cancer Detection Based on incremental Biochemical and Physiological Properties of Breast Cancers: A Six-Year, Two-Site Study," *Acad. Radiol.* **12**,925-933 (2005)
3. Q. Zhu, E. B. Cronin, et al, "Benign versus malignant breast masses: optical differentiation with US-guided optical imaging reconstruction," *Radiology* **237**, 57–66 (2005)
4. Q. Zhu, S. Tannenbaum, et al, "Noninvasive monitoring of breast cancer during neoadjuvant chemotherapy using optical tomography with ultrasound localization," *Neoplasia* **10**(10), 1028-1040 (2008)
5. R. Saxena, T. S. Keller, et al, "A three dimensional finite element scheme to investigate apparent mechanical properties of trabecular bone," *Comp. Meth. Biomech.Biomed. Eng.* **2,** 285-294 (1999)
6. Brian W. Pogue, Shireen Geimer, et al, "Three-dimensional simulation of near-infrared diffusion in tissue: boundary condition and geometry analysis for finite-element image reconstruction," *Applied Optics* **40**(4), 588-600 (2001)
7. L. Wang, S. L. Jacques, et al, "MCML-Monte Carlo modeling of light transport in multi-layered tissues," *Computer Methods and Programs in Biomedicine* **47**, 131-146 (1995)
8. C. Xu and Q. Zhu, "Light Shadowing Effect of Large Breast Lesions Imaged by Optical Tomography in Reflection Geometry," *J. Biomed. Opt.* **15**(3): 036003 1-16 (2010)
9. Spirou G, Oraevsky A, et al, "Optical and acoustic properties at 1064 nm of polyvinyl chloride-plastisol for use as a tissue phantom in biomedical optoacoustics," *Phys. Med. Biol.* **50**, N141-N153 (2005)